

# In vivo multiplexed interrogation of amplified genes identifies GAB2 as an ovarian cancer oncogene

Gavin P. Dunn<sup>a,b,c,d,1</sup>, Hiu Wing Cheung<sup>b,d,1</sup>, Pankaj K. Agarwalla<sup>a,b,c,f</sup>, Sapana Thomas<sup>d</sup>, Yulia Zektser<sup>d</sup>, Alison M. Karst<sup>b,e</sup>, Jesse S. Boehm<sup>d</sup>, Barbara A. Weir<sup>d</sup>, Aaron M. Berlin<sup>d</sup>, Lihua Zou<sup>d</sup>, Gad Getz<sup>d</sup>, Joyce F. Liu<sup>b,f</sup>, Michelle Hirsch<sup>g</sup>, Francisca Vazquez<sup>d</sup>, David E. Root<sup>d</sup>, Rameen Beroukhim<sup>b,c,d,f,h</sup>, Ronny Drapkin<sup>b,e,g</sup>, and William C. Hahn<sup>b,d,f,h,2</sup>

<sup>a</sup>Department of Neurosurgery, Massachusetts General Hospital, Harvard Medical School, Boston, MA 02114; <sup>b</sup>Department of Medical Oncology, <sup>c</sup>Center for Cancer Genome Discovery, <sup>d</sup>Cancer Biology, and <sup>e</sup>Center for Molecular Oncologic Pathology, Dana-Farber Cancer Institute, Harvard Medical School, Boston, MA 02215; <sup>f</sup>Broad Institute of Harvard and Massachusetts Institute of Technology, Cambridge, MA 02142; and Departments of <sup>g</sup>Medicine and <sup>h</sup>Pathology, Brigham and Women's Hospital and Harvard Medical School, Boston, MA 02115

Edited\* by Robert D. Schreiber, Washington University School of Medicine in St. Louis, St. Louis, MO, and approved November 25, 2013 (received for review July 9, 2013)

High-grade serous ovarian cancers are characterized by widespread recurrent copy number alterations. Although some regions of copy number change harbor known oncogenes and tumor suppressor genes, the genes targeted by the majority of amplified or deleted regions in ovarian cancer remain undefined. Here we systematically tested amplified genes for their ability to promote tumor formation using an in vivo multiplexed transformation assay. We identified the GRB2-associated binding protein 2 (GAB2) as a recurrently amplified gene that potently transforms immortalized ovarian and fallopian tube secretory epithelial cells. Cancer cell lines overexpressing GAB2 require GAB2 for survival and show evidence of phosphatidylinositol 3-kinase (PI3K) pathway activation, which was required for GAB2-induced transformation. Cell lines overexpressing GAB2 were as sensitive to PI3K inhibition as cell lines harboring mutant *PIK3CA*. Together, these observations nominate GAB2 as an ovarian cancer oncogene, identify an alternative mechanism to activate PI3K signaling, and underscore the importance of PI3K signaling in this cancer.

functional genomics | open reading frame | ORF

Several histologic subtypes are associated with unique biological behaviors collectively called “ovarian cancer,” and serous tumors represent the majority of high-grade serous ovarian epithelial (HGSOE) cancers (1). The Cancer Genome Atlas (TCGA) has performed a large-scale, multiplatform genomic profiling study of primary HGSOE cancers, and the gene expression analysis from this study and others (2) demonstrated that at least four different molecular subtypes comprise clinically defined high-grade serous and endometrioid ovarian cancer. Genomic characterization of these tumors revealed ubiquitous copy number alterations as the dominant genetic alterations in ovarian cancer and a surprisingly small number of recurrent, significant mutations (3). Although these efforts confirmed recurrent copy number alterations in well-acknowledged driver genes, such as *MYC* and *CCNE1*, in a subset of serous ovarian cancers, the identity of the driver genes resident in the majority of the 63 focal and recurrent regions of amplification remain undefined.

Functional interrogation of somatically altered genes represents a complementary approach to large-scale structural genome characterization. We and others have performed large scale, loss-of-function short hairpin RNA (shRNA) screens to identify essential cancer genes and recently reported *PAX8* and *ID4* as ovarian cancer dependencies (4, 5). In other cancer types, both genome-wide and targeted loss-of-function studies were used to identify novel tumor suppressors in hepatocellular carcinoma (6) and epigenetic regulators in lymphomas (7). In addition, gain-of-function, cDNA-based approaches have uncovered novel driver roles for *IKBKE* (8) and *PAKI* (9) in breast cancer, *ERBB3* in endometrial cancer (10), and *FGF19* in hepatocellular cancer (11). These studies demonstrate the utility of integrating evidence from

both structural and functional assays to identify genes that represent tractable therapeutic targets.

Here we have developed and implemented a multiplexed in vivo transformation assay to identify genes recurrently amplified in HGSOE cancers that suffice to induce tumorigenic growth of immortalized human cells. These observations credential *GAB2* as an ovarian cancer oncogene.

## Results

**Amplicon-Based Pooled in Vivo Transformation Screen.** To identify recurrently amplified genes that contribute to tumorigenicity in HGSOE cancers, we initiated a systematic study in which we used genome characterization data to identify recurrent amplified genes, created a lentivirally delivered collection of ORFs, and then screened for genes that induced tumorigenicity using a multiplexed in vivo transformation assay. We queried the copy number data generated by TCGA (3) to identify 1,017 recurrently amplified genes resident in the 63 recurrently amplified regions in HGSOE cancers. Using the Center for Cancer Systems Biology (CCSB)/Broad Institute lentiviral ORF expression collection (12), we created an arrayed collection of 587 ORFs representing 455 amplified ovarian genes (Dataset S1) including *AKT1* that served as a positive control.

## Significance

High-grade serous ovarian cancers are characterized by widespread gain and loss of copy number involving large numbers of genes; however, the functional consequences of many of these changes remain unclear. To determine which of the many amplified genes exhibited tumor-promoting behavior, we developed a novel in vivo method to systematically screen potential oncogenes for tumor formation. We identified GAB2, a signaling adaptor protein, as a potent oncogene that is also significantly amplified in ovarian and breast cancer. GAB2 overexpression activates the phosphatidylinositol 3-kinase (PI3K) pathway and confers sensitivity to PI3K pathway inhibition. These results credential GAB2 as a potent oncogene in ovarian cancer and emphasize the importance of PI3K signaling in this cancer.

Author contributions: G.P.D., H.W.C., J.S.B., and W.C.H. designed research; G.P.D., H.W.C., P.K.A., S.T., Y.Z., and A.M.K. performed research; B.A.W., A.M.B., L.Z., G.G., D.E.R., R.B., and R.D. contributed new reagents/analytic tools; G.P.D., H.W.C., J.S.B., B.A.W., L.Z., G.G., J.F.L., M.H., F.V., R.B., R.D., and W.C.H. analyzed data; and G.P.D., H.W.C., and W.C.H. wrote the paper.

Conflict of interest statement: R.B. and W.C.H. are consultants to Novartis as noted in this work.

\*This Direct Submission article had a prearranged editor.

<sup>1</sup>G.P.D. and H.W.C. contributed equally to this work.

<sup>2</sup>To whom correspondence should be addressed. E-mail: william\_hahn@dfci.harvard.edu.

This article contains supporting information online at [www.pnas.org/lookup/suppl/doi:10.1073/pnas.1311909111/-DCSupplemental](http://www.pnas.org/lookup/suppl/doi:10.1073/pnas.1311909111/-DCSupplemental).



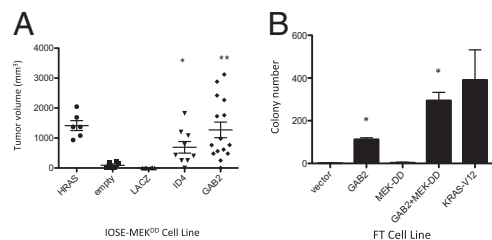


**Fig. 2.** GAB2 overexpression promotes tumor formation. (A) IOSE-MEK<sup>DD</sup> cells alone or expressing *HRAS*<sup>V12</sup>, *ID4*, *LACZ*, or *GAB2* were assessed for tumor formation and tumor volume in *NOD/IL2Rγ<sup>−/−</sup>/Jscid* mice. *P* values for transduced HA1E-M cell lines compared with HA1E-M “empty” cells are the following: HA1E-M-ID4, \**P* = 0.0286; and \*\*HA1E-M-GAB2, *P* = 0.0110. (B) Immortalized FTSECs transduced with empty vector, *GAB2*, MEK<sup>−DD</sup>, *GAB2* + MEK<sup>−DD</sup>, or *HRAS*<sup>V12</sup> were grown in soft agar and assessed for colony formation. *P* values for transduced FTSECs compared with FTSECs transduced with vector alone are \**P* < 0.0001 for FT-GAB2 and FT-GAB2-MEDK<sup>−DD</sup>. Error bars in A and B show standard deviation.

GAB2 protein levels by reverse phase protein array (RPPA). Of 326 analyzed samples, 58 of 326 (18%) displayed elevated protein expression and harbored elevated gene expression, gene amplification, or both characteristics (Fig. 3C). Of these high-expressing samples, 14 demonstrated the highest level of expression and were defined by both high *GAB2* gene amplification and elevated levels of *GAB2* mRNA. Having documented GAB2 overexpression by RPPA, we performed an independent analysis of protein expression via immunohistochemical analysis of GAB2 expression in tissue microarrays (TMAs) generated from patients with high-grade serous ovarian adenocarcinoma. Of 132 tumors assessed, we found 89 of 132 (67%) to be GAB2-negative with staining scores of 0 or 1+ (Fig. 3D). However, 43 of 132 (33%) samples were GAB2-positive (scores 2+ and 3+), with expression predominantly noted in the cytoplasm. These findings paralleled what we observed using RPPA. Finally, using the copy number and expression data in the Cancer Cell Line Encyclopedia (23), we identified ovarian cancer cell lines in which GAB2 was amplified and overexpressed (ONCODG1 and NIH:OVCAR3) and not amplified but overexpressed (IGROV1 and FUVO1). In contrast, the OV56 ovarian and MDA-MB-453 breast cancer cell lines expressed low levels of GAB2 (Fig. 3E). The lower molecular weight GAB2 seen in ONCODG1 and NIH:OVCAR3 likely represents a smaller isoform of GAB2 that lacks the first exon of the *GAB2* gene and is likely translated from an internal methionine of the second exon (Fig. S1). Together, these results show that *GAB2* is a significant target of amplification in human ovarian cancer and is both amplified and also overexpressed in human cancer cell lines and primary tumor samples.

**Ovarian Cancer Cell Dependency on GAB2.** The finding that GAB2 induced tumorigenicity and is amplified and overexpressed in a subset of ovarian cancers suggested that *GAB2* was one target of the 11q14 amplicon. We investigated whether cell lines that harbor *GAB2* amplification and/or overexpression required GAB2 expression for proliferation to establish that *GAB2* is one target of the amplicon on chromosome 11q. We used a panel of ovarian cancer cell lines that overexpress GAB2 (NIH:OVCAR3, FUVO1, and IGROV1) and representative ovarian (OV56) and breast (MDA-MB-453) cancer cell lines with low GAB2 expression and expressed two independent shRNAs targeting *GAB2* or a control shRNA construct targeting *LACZ* (shLACZ, Fig. 4A). Cell lines that overexpress GAB2 exhibited significantly decreased proliferation compared with cells expressing the shRNA targeting *LACZ* (Fig. 4B). In contrast, suppression of representative cell lines with low GAB2 expression failed to inhibit cell proliferation. Although these observations are representative of a range of cell lines tested, we also identified a subset of cell lines with lower GAB2 expression that were sensitive to GAB2 suppression (Fig. S2A and B), likely due to the involvement of GAB2 in other cancer-relevant signaling

pathways such as those driven by receptor tyrosine kinases. These observations support the notion that GAB2 represents a dependency in GAB2-altered ovarian cancer cell lines.

**Signaling Pathways Activated by GAB2.** Prior work has implicated GAB2 as a signaling intermediate in both SHP2-dependent activation of MAPK signaling (16, 17) and activation of phosphatidylinositol 3-kinase (PI3K) (24). To assess the effects of suppressing *GAB2* on these signaling pathways in cell lines expressing elevated or normal levels of GAB2, we interrogated the phosphorylation levels of PI3K/AKT/mTOR pathway components AKT1 and S6 as well as the MAPK pathway component ERK. When we suppressed GAB2 with 2 independent *GAB2*-specific shRNAs in NIH:OVCAR3 and FUVO1 cell lines, we found decreased levels of phospho-AKT1, phospho-S6, and phospho-ERK1/2 compared with cells expressing a control shRNA, shLacZ (Fig. 4C). In contrast, suppression of *GAB2* in the MDA-MB-453 and BT20 cell lines, both of which express lower levels of GAB2 and also harbor *PIK3CA* mutations, failed to induce changes in the observed levels of phospho-AKT1 or phospho-S6, and induced only a minimal decrease in phospho-ERK1/2 levels. Also, suppression of *GAB2* in two additional low-expressing lines, OV7 and OVK18, failed to induce changes in pathway activation (Fig. S2A). These observations suggest that the PI3K/AKT1/mTOR and MAPK pathways are activated by GAB2 selectively in cell lines that overexpress this protein.

**PI3K Activation in GAB2-Mediated Transformation/Dependency.** “PI3Kness” appears to be a critical feature of both type I and type II ovarian cancers (25). However, analysis of the TCGA dataset revealed that alterations in known PI3K pathway components including *PTEN*, *PIK3CA*, *AKT1*, and *AKT2* were present in only about one-third of ovarian cancer samples (3). Although prior studies have shown that GAB2-mediated migration of melanoma (24) and ovarian cancer cells (26) can be reduced by PI3K inhibitors, we hypothesized that *GAB2*

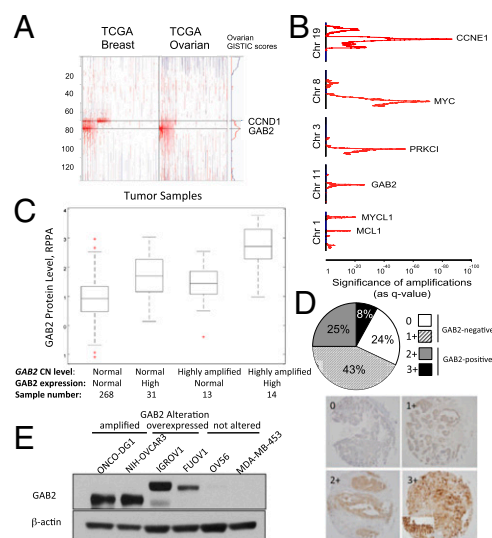


**Fig. 3.** Amplification and overexpression of GAB2 in human ovarian cancers. (A) GISTIC analysis of TCGA copy number data showing *GAB2* amplification on 11q14. Regions of amplification and deletion are shown in red and blue, respectively. (B) Ranking of gene peak regions of amplification in ovarian cancer by significance value analysis. (C) RPPA of TCGA ovarian cancer samples by copy number and gene expression levels. Box plots include values comprising the 25th–75th percentiles, and bars extend to extreme data values; red crosses are outliers. (D) Immunohistochemical analysis of GAB2 expression in ovarian cancer TMAs. Scores were assigned based on staining intensity: 0 (negative), 1 (weak), 2 (moderate), and 3 (strong) intensity. (E) Immunoblot analysis of GAB2 protein expression in ONCO-DG1, NIH:OVCAR3, IGROV1, FUVO1, OV56, and MDA-MB-453 cell lines.

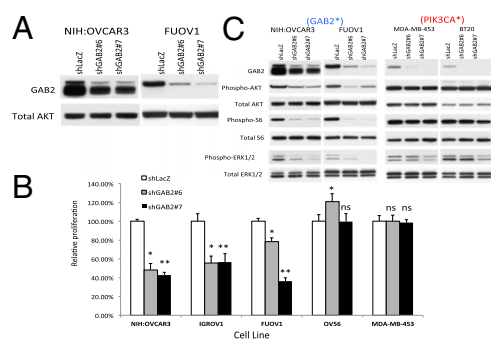


**Fig. 4.** Effects of suppressing *GAB2* expression. (A) Suppression of *GAB2* by two independent *GAB2*-specific shRNAs, shGAB2 #6 and shGAB2 #7, in ovarian cancer cell lines NIH:OVCAR3 and FUOV1. (B) Effects of suppressing *GAB2* expression on cell proliferation in a panel of ovarian, lung, and breast cancer cell lines that include high-expressing (NIH:OVCAR3, FUOV1, IGROV1, COV-362, NCI-H1435) and low-expressing (MDA-MB-453) cell lines. Statistically significant *P* values for cells expressing shGAB2 #6 (\*) and shGAB2 #7 (\*\*) compared with shLacZ control for each cell line are the following: NIH:OVCAR3, \**P* < 0.0001 and \*\**P* < 0.0001; IGROV1, \**P* < 0.0001 and \*\**P* < 0.0001; FUOV1, \**P* < 0.05 and \*\**P* < 0.0001; OV-56, shGAB2 #6 *P* < 0.0001 and shGAB2 #7 *P* = 0.8617; MD-MB-453, shGAB2 #6 *P* = 0.9847 and shGAB2 #7 *P* = 0.708 calculated by unpaired *t* test. (C) MAPK/ERK and PI3K pathway status following suppression of *GAB2*. GAB2\*, *GAB2* overexpressing; ns, not significant; PIK3CA\*, PIK3CA mutant.

amplification represents an additional mechanism of PI3K activation in ovarian cancer. We tested whether increased *GAB2* expression activated AKT1. *GAB2* overexpression in IOSE cells led to increased serine 473 phosphorylation of AKT1 compared with IOSE cells expressing control LacZ or the *GAB2*-3YF mutant protein, which impairs the ability of *GAB2* to recruit p85 (Fig. 5A). These observations show that increased *GAB2* levels induced AKT1 phosphorylation, likely via the recruitment of the PIK3CA complex. This phosphorylation event required the activity of the mTOR complex; treatment of IOSE cells overexpressing *GAB2* with Torin2, an inhibitor of both the mTORC1 and mTORC2 complexes (27), abrogated AKT1 phosphorylation by *GAB2*. These data suggest that the mTOR complex is also required for the *GAB2*-mediated activation of AKT1. Having demonstrated that *GAB2* activates AKT1 in a p85 and mTOR-dependent manner, we next tested whether *GAB2*-mediated AKT1 activation was necessary for the transformation of FTSEC. Compared with control FTSECs expressing only the activated *MEK*<sup>DD</sup> allele, FTSEC overexpressing *MEK*<sup>DD</sup> and *GAB2* formed 90-fold more anchorage-independent colonies (Fig. 5B). We then tested the contributions of components of the PI3K pathway contributions to *GAB2*-mediated transformation using two approaches. First, FTSEC expressing both *MEK*<sup>DD</sup> and the p85-binding mutant *GAB2*-3YF formed significantly fewer colonies than WT *GAB2*-expressing cells. Secondly, FTSEC expressing *MEK*<sup>DD</sup> as well as WT *GAB2* formed background levels of colonies when treated with the PI3K inhibitor GDC-0491 at 1  $\mu$ M. In contrast, overexpression of a *GAB2* mutant protein with impaired Shp2 binding failed to impair transformation in the HA1EM background. Together, these data show that PI3K pathway activation is required for *GAB2*-mediated transformation in a model of ovarian cancer using physiologically relevant cells of origin.

We extended these observations by exploring whether independent activation of the downstream PI3K/AKT pathway could rescue cells dependent upon *GAB2* function in which *GAB2* levels had been suppressed. We introduced a myristoylated, constitutively active form of AKT1 (myrAKT1) or a control vector into NIH:OVCAR3 cells and subsequently expressed a control *lacZ* shRNA or four independent *GAB2*-specific shRNAs and examined for differences in cell proliferation. Compared with GFP-expressing NIH:OVCAR3 cells in which we had

suppressed *GAB2*, NIH:OVCAR3 cells overexpressing constitutively active myrAKT1 showed an  $\sim$ 20% increase in proliferation that was statistically significant with each *GAB2*-specific shRNA tested (Fig. 5C). These observations suggest that *GAB2* likely acts, at least in part, through AKT1.

Finally, because *GAB2* activates the PI3K pathway, we investigated the pattern of genomic alterations of PI3K signaling in primary ovarian cancers. Hanrahan et al. (28) recently reported a substantial number of PI3K pathway alterations in ovarian cancer. We extended this analysis by analyzing a substantially larger number the number of samples and also incorporating *GAB2* in our analysis. Specifically, we analyzed the ovarian cancer TCGA dataset to determine the incidence and type of alterations in *PIK3CA*, *PIK3CB*, *GAB2*, *AKT1*, *AKT2*, *AKT3*, *PTEN*, and *PDK1*. Of the 562 samples analyzed, we found that nearly 54% harbored significant copy number alterations or mutations in these genes. Similar to our prior analysis, 13% of samples harbored *GAB2* amplifications, some of which co-occurred with amplification of other pathway components. These observations suggest that amplification of *GAB2* also leads to activation of PI3K signaling.

**Sensitivity of *GAB2*-Altered Cell Lines to PI3K Inhibition.** Having shown that the PI3K pathway was required for *GAB2*-mediated transformation and that activated AKT1 could partially rescue *GAB2*-dependent cell lines depleted of *GAB2*, we next determined whether *GAB2* alterations represented a feature that correlated with enhanced sensitivity to PI3K pathway inhibition. Several studies suggest that PI3K inhibition attenuated *GAB2*-dependent migration phenotypes (24, 26) and pointed to the types of pathway alterations that activate AKT1 (28). However, although recent work has been directed at correlating PI3K pathway alterations with sensitivity to pathway inhibition in breast cancer (29), it is unclear whether increased *GAB2* expression increases cell sensitivity to PI3K pathway inhibition in a manner similar to the sensitivity conferred by canonical mutations in *PIK3CA* and *PTEN*. We performed dose-response experiments to determine the IC<sub>50</sub> of inhibitors against PI3K (GDC-0941) or MEK1 (AZD-6244) in a panel of 12 ovarian and 11 breast cancer cell lines 3 d posttreatment. In *GAB2*-overexpressing cell lines, GDC-0941 treatment abolished levels of both phospho-AKT1 and phospho-S6, and AZD-6244 treatment abolished phospho-ERK 1/2 (Fig. 6A). We observed similar effects in cell lines with low *GAB2* expression (Fig. S24). We observed that 10 cell lines that harbored amplification/overexpression of *GAB2* formed a distinct subgroup from 9 cell lines that harbored mutation of *PIK3CA* or loss of *PTEN*, with the

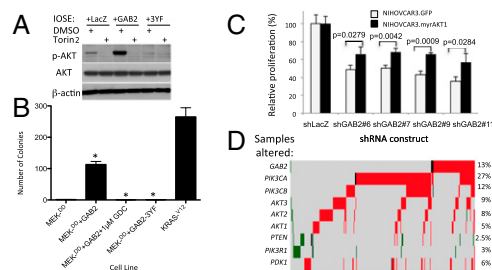


**Fig. 5.** Effects of *GAB2* expression on activation of the PI3K signaling. (A) mTOR-mediated phosphorylation of AKT following *GAB2* expression in IOSE cell lines. (B) PI3K dependence of transformed FTSECs expressing *GAB2*. FTSECs overexpressing wild-type *GAB2* were treated with PI3K inhibitor GDC-0941. Overexpression of the *GAB2* p85 binding mutant (*GAB2*-3YF) was also tested. \**P* < 0.0001. (C) Rescue of *GAB2* knockdown in NIH:OVCAR3 by overexpressing myristoylated, constitutively active AKT1. (D) Heat map of TCGA ovarian cancer samples with alterations in *GAB2*, *PIK3CA*, *AKT1*, or *PTEN* demonstrating statistically significant mutual exclusivity of *GAB2* amplification and either *PIK3CA* amplification or *PTEN* loss. Red bars indicate amplification, black bars indicate mutation, and green bars indicate deletion. In C and D, error bars reflect standard deviation.

exception of IGROV1 cells that harbor both loss of *PTEN* and overexpression of *GAB2* (Fig. 6B). Using nonlinear regression followed by comparison of the best-fit parameters, we found that the mean  $IC_{50}$  of GDC-0941 were comparable between the cell lines harboring amplification/overexpression of *GAB2* ( $0.485 \pm 0.553 \mu\text{M}$ ) and the cell lines harboring activating mutations of *PIK3CA* or loss of *PTEN* ( $0.583 \pm 1.032 \mu\text{M}$ ). In contrast, the five cell lines with normal *GAB2* or *PIK3CA/PTEN* exhibit significantly higher  $IC_{50}$  of GDC-0941 (mean  $\pm$  SD =  $8.3 \pm 3.1 \mu\text{M}$ ) compared with cell lines with alterations in *GAB2* or *PIK3CA/PTEN*. These observations suggest that *GAB2*-overexpressing cell lines exhibit sensitivity to PI3K pathway inhibition that is similar to cell lines harboring other PI3K pathway alterations.

## Discussion

Here we screened 455 genes amplified in ovarian cancer for the ability to transform an immortalized human cancer cell line using a pooled high-throughput in vivo approach and identified 26 genes that induced tumorigenicity. We demonstrated that *GAB2* induces the transformation of ovarian and fallopian tube cells by activating PI3K signaling. Ovarian cell lines that harbor *GAB2* amplifications or overexpress *GAB2* are dependent on *GAB2* for proliferation and exhibit sensitivity to PI3K inhibition. These observations identify *GAB2* as an ovarian cancer oncogene and underscore the importance of PI3K signaling in ovarian cancer.

**Multiplexed in Vivo Transformation Screens.** We used a human embryonic kidney cell line expressing the activated *MEK-DD* gene to facilitate a high-throughput, stringent in vivo transformation screen. This model is useful due to its rapid in vivo growth kinetics for oncogene discovery and its low background transformation rate. The HA1E-M model expresses an active MEK allele, thereby facilitating the identification of PI3K-activating genes such as *GAB2*. Further systematic follow-up will be necessary to validate additional candidate oncogenes identified using this system that may vary in strength of transforming capacity. We note that *GAB2* also induced transformation in both ovarian and fallopian tube epithelial cells indicating that the HA1E-M model enabled the identification of ovarian cancer drivers. Additional oncogenes may be uncovered if screened in a cellular context emphasizing other signaling cascades. Although we describe a gain-of-function approach focused on oncogene discovery in ovarian cancer, this methodology can be applied to any cancer phenotype. We used a next-generation sequencing approach that allowed us both to identify ORFs within tumors and quantitate their enrichment. This approach could be applied easily to a range of scalable ORF-expressing pool sizes and phenotypic readouts using ORF collections that do not require additional barcoded cassettes. The observation that one of the three *GAB2*-scoring tumors displayed a lower level of *GAB2* enrichment is likely due to the stochastic selection of clones that

eventually form tumors at each site, owing either to a slight variation in starting pooled inoculum or interactions with the local microenvironment. In addition to *GAB2*, we also identified additional candidates, such as *NARF* and *ASB10*, as genes that induced tumors when overexpressed in HA1E-M cells that merit further investigation. Taken together, these studies provide further evidence that large-scale functional genomics approaches complement ongoing structural approaches to decipher genes and pathways involved in cancer pathogenesis.

**Features of the 11q14 Amplicon.** *GAB2* resides on the fourth most significant amplicon in high-grade serous ovarian cancer (3), the focal peak located on 11q14.1. This amplified region has been identified as a recurrent alteration in breast (9, 22) and ovarian cancer (19) as well as in metastatic melanoma (24). Across over 6,300 different TCGA samples, this region is among the 26 most amplified regions in all cancers (21). This amplicon is slightly broader in breast cancer, encompassing both *GAB2* and *PAK1* (9, 21) as well as the nearby region harboring *CCND1*. Whereas *GAB2* amplification does not appear to be correlated with survival, there is a significant association with *GAB2* amplification and the Her2-enriched ( $P = 0.042$ ) and luminal B ( $P = 0.028$ ) breast cancer subsets described by TCGA. In ovarian cancer, the 11q14.1 amplicon is at smaller and centered over *GAB2*. Although prior studies in ovarian cancer have highlighted the 11q14.1 amplification (3, 19), the identities of the candidate gene targets of amplification were not well clarified. These studies do not preclude the possibility that several genes on the same amplicon may cooperate to drive oncogenic programs. *GAB2* may also contribute to the pathogenesis of individual ovarian cancers in which the center of the region of copy number gain does not fall on *GAB2* itself but on neighboring candidate genes, such as *RSF1* (30), *PAK1* (9, 19), or *CCND1*. Also, there are a significant number of samples that harbor elevated *GAB2* gene expression in the absence of amplification, supporting the idea that amplification is one of several mechanisms underlying *GAB2* protein overexpression and tumorigenesis. We note that *GAB2* is somatically mutated in four TCGA samples, although these amino acid changes do not affect known functional domains.

***GAB2* Alterations in Cancer.** *GAB2* plays critical roles in several different cancers. *GAB2* is required for BCR/ABL-mediated transformation in chronic myeloid leukemia (CML) (31) and also HER2-mediated mammary carcinogenesis through ERK activation (16). Moreover, *GAB2* is overexpressed in breast cancer (9, 22) and some metastatic melanomas (24) and promotes survival in breast cancer (22) and migration in both malignancies (17, 24). Several ovarian cancer cell lines also overexpress *GAB2*, which was linked to increased migration and the epithelial-mesenchymal transition (26). Davis et al. also demonstrated that a panel of ovarian cancer cell lines with *GAB2* amplification were susceptible to siRNA-mediated *GAB2* knock-down (32), consistent with our findings. Although these prior studies suggest that *GAB2* expression is altered in cancer, the observations presented herein show that *GAB2* is a bona fide oncogene important for both tumor initiation and maintenance.

***GAB2*-Mediated Signaling and the PI3K Pathway.** Recent work suggests that over 70% of ovarian cancers exhibit activation of the PI3K pathway (33), but there are likely more alterations that influence this pathway than have been identified. We identified PI3K pathway alterations in 54% of the high-grade serous ovarian cancer samples we analyzed from the TCGA dataset. *PIK3CA* amplification was a common event and has been seen in other cancers (34, 35). Co-occurrence of *GAB2* amplification and PI3K pathway component alteration was observed in a subset of ovarian cancer samples. Co-occurrence of altered PI3K pathway components has been observed in other PI3K-altered cancer types and could potentiate PI3K-mediated signaling. Based on our findings, *GAB2* overexpression represents a subset of pathway alterations that result in dysregulated PI3K signaling. Several studies have addressed PI3K/AKT pathway inhibition in

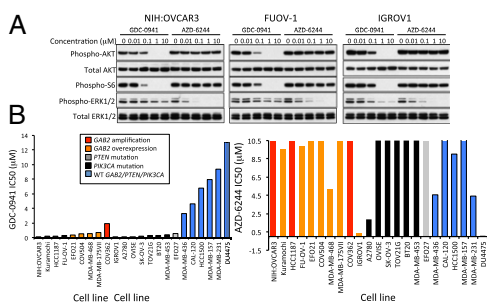


**Fig. 6.** Effects of a PI3K inhibitor on cell proliferation. (A) Effect of increasing doses of the PI3K inhibitor GDC-0941 or the MEK inhibitor AZD-6244 on AKT1, ERK1/2, and S6 phosphorylation in *GAB2*-overexpressing cell lines NIH: OVCA3, FUOV-1, and IGROV1. (B) Half-maximal inhibitory concentrations ( $IC_{50}$ ) for GDC-0941 (Left) and AZD-6244 (Right) in 23 ovarian and breast cancer cell lines. Genomic alterations are depicted by color as shown in *Inset*.

ovarian cancer. In one study, a subset of ovarian cancer cell lines was sensitive to inhibition of AKT1 and AKT2, whereas those expressing AKT3 required inhibition of all three isoforms (28). In a separate study, modest clinical responses were seen in a phase-I trial incorporating mTOR inhibitors in the patients with *PIK3CA* mutant compared with *PIK3CA* wild-type cancers (36). These findings point to the importance of careful genetic annotation in tailoring pathway-specific therapies. Our findings suggest that cell lines characterized as GAB2 overexpressing are as sensitive to PI3K pathway inhibition as cell lines harboring classical *PIK3CA* mutations, and subsequent work has shown that additional cell lines with low GAB2 expression, OV7 and OVK18, exhibit nearly fourfold higher IC<sub>50</sub> values in response to PI3K inhibitor treatment. These observations provide a rationale to consider inhibition of this pathway in human ovarian cancers as well as breast cancers and metastatic melanomas exhibiting appropriate pathway-specific genomic features.

**Adapter Proteins as Therapeutic Targets.** In addition to its ability to activate the PI3K pathway, GAB2 can also activate the ERK pathway through Shp2. In a mammary epithelial cell model, NeuNT-driven multiacinar structure formation through GAB2 requires Shp2/ERK signaling (16). However, we failed to observe a decrease in transformation using a GAB2 mutant unable to bind Shp2 and did not find that ovarian cancer cell lines were as sensitive to MEK inhibition as they were to PI3K inhibition. Together, these observations suggest that signaling events downstream of GAB2 may be context or lineage specific. Further work will be necessary to address these possibilities.

Adapter proteins amplify receptor-initiated signaling events by recruiting downstream modular signaling proteins. Thus, genes such as *GAB2* and *CRKL* (37) are powerful transforming oncogenes because of the number of pathways influenced by their overexpression. As was demonstrated in *CRKL*-overexpressing mutant *EGFR* lung cancer cells resistant to *EGFR* inhibition (37), cells overexpressing GAB2 may be resistant to inhibitors of upstream

receptor tyrosine kinases, such as HER2, with which GAB2 associates. Adaptor proteins may represent a class of cancer-relevant targets that warrant further study. The observation that GAB2 copy number alterations correlate with sensitivity to PI3K pathway inhibition supports the prospective annotation of *GAB2* amplification or elevated GAB2 protein expression in clinical trials of PI3K inhibitors.

## Materials and Methods

**Pooled in Vivo ORF Screen.** Five hundred eighty-eight ORFs representing genes recurrently amplified in the ovarian cancer TCGA dataset as well as controls were obtained from the CCSB/Broad Institute ORF collection (12). HA1E-M cells were infected in arrayed fashion, pooled, and injected into three sites each in two NCr nude mice (Taconic) per pool. Growing tumors were harvested, and ORFs were amplified from genomic DNA and recombined into common vectors, and pooled recombinant plasmids were recovered from transformed bacteria and subjected to next-generation sequencing. Extended details are described in *SI Materials and Methods*.

**Additional Materials and Methods.** Plasmids, cell lines and reagents, chemicals, immunoblotting, cell proliferation and anchorage-independence assays, TMA and immunohistochemistry, genomics/proteomics analysis, and animal injections are described in *SI Materials and Methods*.

**ACKNOWLEDGMENTS.** We thank John Doench, Glenn Cowley, and Carsten Russ from the Broad Institute for helpful discussions. The following grant support is acknowledged: RC2 CA148268 (to W.C.H.), U01 CA176058 (to W.C.H.), U54 CA143798 (to R.B.), U54 CA112962 (to W.C.H.), NIH R25 (to G.P.D.), the American Brain Tumor Association (G.P.D.), a Canadian Institutes of Health Research Fellowship (to A.M.K.), a Kaleidoscope of Hope Foundation Young Investigator Research Award (to A.M.K.), U01 CA152990 (to R.D.), The Mary Kay Foundation (R.D.), The Sandy Rollman Ovarian Cancer Research Foundation (R.D.), The Robert and Debra First Fund (R.D.), The Executive Council of the Susan Smith Center for Women's Cancers at Dana-Farber Cancer Institute (R.D.), The V Foundation for Cancer Research (H.W.C.), American Cancer Society Institutional Research Grant IRG-97-219-14 (to H.W.C.), and The Marsha Rivkin Center for Ovarian Cancer Research (H.W.C.).

- Soslow RA (2008) Histologic subtypes of ovarian carcinoma: An overview. *Int J Gynecol Pathol* 27(2):161–174.
- Tothill RW, et al.; Australian Ovarian Cancer Study Group (2008) Novel molecular subtypes of serous and endometrioid ovarian cancer linked to clinical outcome. *Clin Cancer Res* 14(16):5198–5208.
- Cancer Genome Atlas Network (2011) Integrated genomic analyses of ovarian carcinoma. *Nature* 474(7353):609–615.
- Cheung HW, et al. (2011) Systematic investigation of genetic vulnerabilities across cancer cell lines reveals lineage-specific dependencies in ovarian cancer. *Proc Natl Acad Sci USA* 108(30):12372–12377.
- Ren Y, et al. (2012) Targeted tumor-penetrating siRNA nanocomplexes for credentialing the ovarian cancer oncogene ID4. *Sci Transl Med* 4(147):ra112.
- Zender L, et al. (2008) An oncogenomics-based in vivo RNAi screen identifies tumor suppressors in liver cancer. *Cell* 135(5):852–864.
- Rui L, et al. (2010) Cooperative epigenetic modulation by cancer amplicon genes. *Cancer Cell* 18(6):590–605.
- Boehm JS, et al. (2007) Integrative genomic approaches identify IKBKE as a breast cancer oncogene. *Cell* 129(6):1065–1079.
- Shrestha Y, et al. (2012) PAK1 is a breast cancer oncogene that coordinately activates MAPK and MET signaling. *Oncogene* 31(29):3397–3408.
- Liang H, et al. (2012) Whole-exome sequencing combined with functional genomics reveals novel candidate driver cancer genes in endometrial cancer. *Genome Res* 22(11):2120–2129.
- Sawey ET, et al. (2011) Identification of a therapeutic strategy targeting amplified FGF19 in liver cancer by Oncogenomic screening. *Cancer Cell* 19(3):347–358.
- Yang X, et al. (2011) A public genome-scale lentiviral expression library of human ORFs. *Nat Methods* 8(8):659–661.
- Hahn WC, et al. (2002) Enumeration of the simian virus 40 early region elements necessary for human cell transformation. *Mol Cell Biol* 22(7):2111–2123.
- Counter CM, et al. (1998) Dissociation among in vitro telomerase activity, telomere maintenance, and cellular immortalization. *Proc Natl Acad Sci USA* 95(25):14723–14728.
- Hahn WC, Weinberg RA (2002) Rules for making human tumor cells. *N Engl J Med* 347(20):1593–1603.
- Bentires-Alj M, et al. (2006) A role for the scaffolding adapter GAB2 in breast cancer. *Nat Med* 12(1):114–121.
- Ke Y, et al. (2007) Role of Gab2 in mammary tumorigenesis and metastasis. *Oncogene* 26(34):4951–4960.
- Karst AM, Levanon K, Drapkin R (2011) Modeling high-grade serous ovarian carcinogenesis from the fallopian tube. *Proc Natl Acad Sci USA* 108(18):7547–7552.
- Brown LA, et al. (2008) Amplification of 11q13 in ovarian carcinoma. *Genes Chromosomes Cancer* 47(6):481–489.
- Mermel CH, et al. (2011) GISTIC2.0 facilitates sensitive and confident localization of the targets of focal somatic copy-number alteration in human cancers. *Genome Biol* 12(4):R41.
- The Broad Institute Portal Team (2012) TCGA Copy Number Portal. Available at www.broadinstitute.org/tcga/home. Accessed November 20, 2012 (data freeze).
- Bocanegra M, et al. (2010) Focal amplification and oncogene dependency of GAB2 in breast cancer. *Oncogene* 29(5):774–779.
- Barretina J, et al. (2012) The Cancer Cell Line Encyclopedia enables predictive modelling of anticancer drug sensitivity. *Nature* 483(7391):603–607.
- Horst B, et al. (2009) Gab2-mediated signaling promotes melanoma metastasis. *Am J Pathol* 174(4):1524–1533.
- Bast RC, Jr., Mills GB (2012) Dissecting “PI3Kness”: The complexity of personalized therapy for ovarian cancer. *Cancer Discov* 2(1):16–18.
- Wang Y, Sheng Q, Spillman MA, Behbakht K, Gu H (2012) Gab2 regulates the migratory behaviors and E-cadherin expression via activation of the PI3K pathway in ovarian cancer cells. *Oncogene* 31(20):2512–2520.
- Qiu L, et al. (2013) Characterization of Torin2, an ATP-competitive inhibitor of mTOR, ATM, and ATR. *Cancer Res* 73(8):2574–2586.
- Hanrahan AJ, et al. (2012) Genomic complexity and AKT dependence in serous ovarian cancer. *Cancer Discov* 2(1):56–67.
- O'Brien C, et al. (2010) Predictive biomarkers of sensitivity to the phosphatidylinositol 3' kinase inhibitor GDC-0941 in breast cancer preclinical models. *Clin Cancer Res* 16(14):3670–3683.
- Shih IeM, et al. (2005) Amplification of a chromatin remodeling gene, Rsf-1/HBXAP, in ovarian carcinoma. *Proc Natl Acad Sci USA* 102(39):14004–14009.
- Sattler M, et al. (2002) Critical role for Gab2 in transformation by BCR/ABL. *Cancer Cell* 1(5):479–492.
- Davis SJ, et al. (2013) Functional analysis of genes in regions commonly amplified in high-grade serous and endometrioid ovarian cancer. *Clin Cancer Res* 19(6):1411–1421.
- Bast RC, Jr., Hennessy B, Mills GB (2009) The biology of ovarian cancer: New opportunities for translation. *Nat Rev Cancer* 9(6):415–428.
- Shi J, et al. (2012) Highly frequent PIK3CA amplification is associated with poor prognosis in gastric cancer. *BMC Cancer* 12:50.
- Cancer Genome Atlas Network (2012) Comprehensive molecular portraits of human breast tumours. *Nature* 490(7418):61–70.
- Janku F, et al. (2012) PI3K/AKT/mTOR inhibitors in patients with breast and gynecologic malignancies harboring PIK3CA mutations. *J Clin Oncol* 30(8):777–782.
- Cheung HW, et al. (2011) Amplification of CRKL induces transformation and epidermal growth factor receptor inhibitor resistance in human non-small cell lung cancers. *Cancer Discov* 1(7):608–625.

# Supporting Information

Dunn et al. 10.1073/pnas.1311909111

## SI Materials and Methods

**Plasmids.** All ORFs used in the screen were cloned into the pLX304 vector backbone and obtained from the Center for Cancer Systems Biology (CCSB)/Broad Institute ORF collection (1). The pLX304-GAB2-3YF mutant was generated by serial overlapping site-directed mutagenesis via a protocol similar to that described previously (2). Y452F, Y476F, and Y584F mutations were introduced using the following primers: Y452F-For (5'-CAG CAC CAA TTC TGA AGA CAA CTT TGT GCC CAT GAA-3') and Y452F-Rev (5'-TTC ATG GGC ACA AAG TTG TCT TCA GAA TTG GTG CTG-3'), Y476F-For (5'-ATT CCC AGA GCG TCT TCA TCC CAA TGA GCC C-3') and Y476F-Rev (5'-GGG CTC ATT GGG ATG AAG ACG CTC TGG GAA T-3'), Y584F-For (5'-CAG GAG ACA GCG AAG AGA ACT TTG TCC CTA TGC-3') and Y584F-Rev (5'-GCA TAG GGA CAA AGT TCT CTT CGC TGT CTC CTG-3'), and pLX-for, (5'-CAC CAA AAT CAA CGG GAC TT-3') and pLX-rev (5'-CAA CAC CAC GGA ATT GTC AG-3'). The pLX-LacZ, pLX-KRAS<sup>V12</sup>, and pLX-HRAS<sup>V12</sup> plasmids were obtained from the CCSB/Broad Institute ORF collection. The pLenti6.3-blebbistatin-IDD4 has been described previously (3). Retroviral plasmid pBabe-Puro-MEK<sup>DD</sup> has been described previously (4). The pBabe-GFP-myristoylated AKT1 plasmid was generated by subcloning the myristoylated Flag epitope tagged AKT1 (myr-Flag-AKT1) cassette (4) into the pBabe-GFP vector (Addgene plasmid 10668). All short hairpin RNA (shRNA) constructs were obtained from The RNAi Consortium (Broad Institute, Cambridge, MA) and have the following clone reference numbers: shLacZ (TRCN0000231710), shGAB2 #6 (TRCN0000155921), shGAB2 #7 (TRCN0000154991), shGAB2 #9 (TRCN0000155271), and shGAB2 #10 (TRCN0000154706).

**Cell Lines and Reagents.** Immortalized human embryonic kidney epithelial cells overexpressing MEK<sup>DD</sup> (HA1E-M) cells (4), immortalized fallopian tube secretory epithelial cells (FTSECs) (5), and immortalized ovarian surface epithelial (IOSE) cells (6) were described previously. NCI-H1435 and MDA-MB-468 cell lines were purchased from the American Type Culture Collection. NIH-OVCAR3, COV362, FUOV1, IGROV1, MDA-MB-453, BT20, A2780, HCC1187, OVCAR8, Kuramochi, EFO21, COV504, OVISE, SK-OV-3, TOV21G, and EFO27 were genotyped at the Broad Institute (7). All cell lines were maintained in DMEM (Mediatech) supplemented with 10% (vol/vol) FBS (Sigma-Aldrich) and 1% penicillin/streptomycin (Cellgro).

**Pooled in Vivo ORF Screen.** The 588 ORFs representing genes amplified in the ovarian cancer The Cancer Genome Atlas (TCGA) dataset as well as positive and negative controls were obtained from the CCSB/Broad Institute ORF collection. HA1E-M cells were plated at a density of 6,800 cells per well in 96-well flat-bottom plates (VWR) and infected in arrayed fashion with lentivirus generated from the lentiviral ORF plasmids. After 2 d, singly infected confluent wells were pooled into collections of 22–24 ORF-expressing HA1E-M cells, expanded into T-150 tissue culture flasks (VWR), and injected. Positive controls 1:24 and 15:24 mixtures of pLX304-AKT1-infected HA1E-M cells with uninfected cells as well as a mixture of HA1E-M cells infected with pLX304-BRAF<sup>V600E</sup>, pLX304-KRAS<sup>V12</sup>, or pLX304-HRAS<sup>V12</sup>. Negative controls included a 1:24 mixture of pLX304-EGFP-infected HA1E-M cells with uninfected HA1E-M cells. A replicate of infected HA1E-M cells was treated with 8  $\mu$ g/mL blebbistatin and monitored for cell death. Each pool of HA1E-M

cells was injected into three sites each in two NCr nude mice (Taconic) per pool. Cells were trypsinized, resuspended in PBS, and injected at a concentration of  $10 \times 10^6$  cells per mL in 200  $\mu$ L ( $2 \times 10^6$  cells) per site.

**Identification of ORF Sequences in Tumors.** Tumors were resected when they reached a minimum largest diameter of 1 cm. Tumors were minced to homogeneity in culture medium, and genomic DNA was isolated from two independent tissue sections using the DNeasy Blood & Tissue Kit (Qiagen). ORF sequences were amplified by PCR from 150 ng genomic DNA by amplifying across the ORF sequence using pLX304-specific flanking primers pLX-for and pLX-rev for 35 cycles using KOD polymerase (EMD Millipore). PCR amplicons were purified using the QIAquick PCR Purification Kit (Qiagen), and 200 ng of purified amplicon DNA from each single reaction were cloned into 150 ng of the pDONR223 vector (Invitrogen) using the BP reaction (Invitrogen) for 4 h at room temperature. DH5 $\alpha$  *Escherichia coli* cells were transformed with the entire reaction and plated on LB agar plates containing 50  $\mu$ g/mL spectinomycin. After 12 h, bacterial cells were harvested by scraping, and pDONR223 plasmids harboring recombinant ORF sequences were purified using the QIAprep Spin Miniprep Kit (Qiagen). The pDONR223 ORF plasmids from each tumor were sheared, barcoded, pooled, and sequenced on a HiSeq system (Illumina). ORF incidence per tumor was calculated by dividing the number of duplicated ORF reads by the total number of nonvector duplicated ORF reads in a given pool. ORFs were scored as present if they comprised at least 0.1% of the nonvector sequences.

**Chemicals.** GDC-0941 and AZD-6244 were purchased from Selleck Chemicals. Torin 2 was obtained from Tocris Bioscience.

**Immunoblotting.** Immunoblotting was performed as described (8). Antibodies to the following proteins used for immunoblotting were purchased from Cell Signaling: GAB2 (no. 3239), AKT (no. 9272), phospho-S473 AKT (no. 4060L), mTOR (no. 2972), S6 kinase (no. 9202), phospho-S6 kinase (no. 9205), ERK1/2 (no. 9102), and phospho-ERK1/2 (no. 9101). Additional antibodies for immunoprecipitation and immunoblotting GAB2 included an anti-C-terminal antibody (no. sc-9313, Santa Cruz) and an anti-N-terminal antibody (no. AP6908a, Abgent). Antibody to  $\beta$ -actin (sc-47778) was purchased from Santa Cruz Biotechnology.

**Cell Proliferation Assay.** The 1,700 IGROV1, FUOV1, and OV56 cells; 1,500 NIH:OVCAR3; 2,000 OV7 and OVK18; and 3,000 MDA-MB-453 cells were seeded into each well of 96-well plates 24 h before infection. Six replicate infections were performed for control shRNAs targeting LacZ (shLacZ) and GAB2-specific shRNAs in the presence of 4  $\mu$ g/mL polybrene for 24 h followed by selection with 2  $\mu$ g/mL puromycin. The ATP content was measured at 6 d postinfection by using the CellTiter-Glo luminescent cell viability assay (Promega).

**Anchorage-Independent Growth Assay.** Growth in soft agar was determined by plating  $1 \times 10^4$  cells in triplicate in 5 mL medium containing 0.4% Noble agar (BD Biosciences) which was placed on top of 4 mL solidified 0.6% agar. Colonies greater than 100  $\mu$ m in diameter were counted 4 wk after plating.

**High-Density Tissue Microarray and Immunohistochemistry.** A tissue microarray (TMA) comprised 134 cases of high-grade, late-stage ovarian serous carcinoma as well as immunohistochemistry methods

were described previously (9, 10). For immunohistochemistry, antibody to human GAB2 (sc-9313, Santa Cruz Biotechnology) was used at a dilution of 1:500. GAB2 staining was scored on a scale of 0 (negative), 1 (weak), 2 (moderate), and 3 (strong) intensity. All tissue review was performed in a blinded manner by pathologists.

**Analysis of Primary Human TCGA Genomics and Reverse Phase Protein Array Data.** We used the Broad Institute Firehose analysis run from August 25, 2012, which may be found in the TCGA Data Coordination Center (<https://confluence.broadinstitute.org/display/GDAC/Home>), for all primary cancer data files (copy number, expression, protein levels) and analysis results [Genomic Identification of Significant Targets in Cancer (GISTIC) result files]. Screenshots of the segmented primary breast and ovarian cancer copy number data (from Affymetrix SNP6 arrays) with scores from TCGA ovarian specific GISTIC analysis were taken using the Integrative Genome Viewer ([www.broadinstitute.org/igv/](http://www.broadinstitute.org/igv/)).

A total of 326 primary ovarian cancer samples from TCGA had reverse phase protein array (RPPA), mRNA expression and copy number data available. GAB2 mRNA levels were pulled from mRNA expression data, using Agilent G4502A arrays. High expression was defined as 1 SD above the mean of GAB2. Protein levels of GAB2 were determined from RPPA arrays. Amplification of GAB2 was pulled from the ovarian cancer GISTIC

results; only those amplifications larger than the arm level amplifications observed for the sample were considered highly amplified.

To analyze GAB2 and additional components of the phosphatidylinositol 3-kinase (PI3K) pathway, copy number pipeline methodology developed at the Broad Institute was applied to the copy number data obtained on the Affymetrix platform across 481 OV samples from the TCGA study deposited at Broad Genome Data Analysis Center (GDAC) Firehose database. We called high-level somatic copy number alternations based on GISTIC 2.0 (11) for GAB2 and the PI3K pathway genes *PIK3CA*, *PIK3CB*, *AKT1*, *AKT2*, *AKT3*, *PTEN*, *PIK3R1*, and *PDK1*.

**Animal Injections/Tumorigenicity.** Cell line xenograft experiments were performed as described (4, 8). Animal protocols were approved by the Dana-Farber Cancer Institute Institutional Care and Use Committee. HA1E-M cells were grown as described above, trypsinized, resuspended in PBS, and injected s.c. at an inoculum of  $2 \times 10^6$  cells per site in 6-wk-old Ncr-nude mice (Taconic). IOSE-derived cells were grown as described above, resuspended in 400  $\mu$ L 1 $\times$  PBS mixed with 400  $\mu$ L of Matrigel Basement Membrane Matrix (BD Biosciences), and injected s.c. at an inoculum of  $2 \times 10^6$  cells per site in 6-wk-old *NOD/IL2R $\gamma$ <sub>c</sub>/scid* mice (Taconic) and monitored for tumor formation.

1. Yang X, et al. (2011) A public genome-scale lentiviral expression library of human ORFs. *Nat Methods* 8(8):659–661.
2. Atanassov II, Atanassov II, Etchells JP, Turner SR (2009) A simple, flexible and efficient PCR-fusion/Gateway cloning procedure for gene fusion, site-directed mutagenesis, short sequence insertion and domain deletions and swaps. *Plant Methods* 5:14.
3. Ren Y, et al. (2012) Targeted tumor-penetrating siRNA nanocomplexes for credentialing the ovarian cancer oncogene ID4. *Sci Transl Med* 4(147):ra112.
4. Boehm JS, et al. (2007) Integrative genomic approaches identify IKBKE as a breast cancer oncogene. *Cell* 129(6):1065–1079.
5. Karst AM, Levanon K, Drapkin R (2011) Modeling high-grade serous ovarian carcinogenesis from the fallopian tube. *Proc Natl Acad Sci USA* 108(18):7547–7552.
6. Liu J, et al. (2004) A genetically defined model for human ovarian cancer. *Cancer Res* 64(5):1655–1663.
7. Cheung HW, et al. (2011) Systematic investigation of genetic vulnerabilities across cancer cell lines reveals lineage-specific dependencies in ovarian cancer. *Proc Natl Acad Sci USA* 108(30):12372–12377.
8. Cheung HW, et al. (2011) Amplification of CRKL induces transformation and epidermal growth factor receptor inhibitor resistance in human non-small cell lung cancers. *Cancer Discov* 1(7):608–625.
9. Claus A, et al. (2010) Overexpression of elafin in ovarian carcinoma is driven by genomic gains and activation of the nuclear factor kappaB pathway and is associated with poor overall survival. *Neoplasia* 12(2):161–172.
10. Liu JF, Hirsch MS, Lee H, Matulonis UA (2009) Prognosis and hormone receptor status in older and younger patients with advanced-stage papillary serous ovarian carcinoma. *Gynecol Oncol* 115(3):401–406.
11. Mermel CH, et al. (2011) GISTIC2.0 facilitates sensitive and confident localization of the targets of focal somatic copy-number alteration in human cancers. *Genome Biol* 12(4):R41.

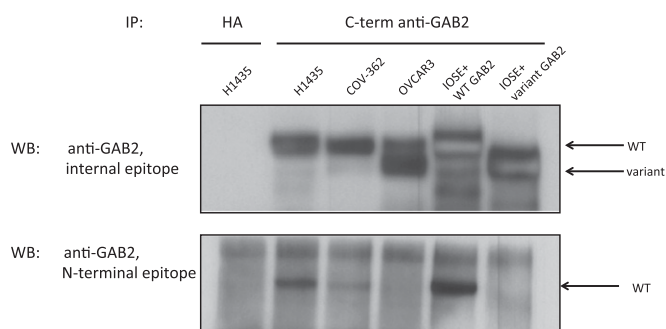


**Fig. S1.** GAB2 isoform expression. GAB2 immune complexes were isolated from NCI-H1435, COV-362, and OVCA93 cells as well as IOSE cells overexpressing the wild-type (WT) full-length isoform of GAB2 or the variant isoform of GAB2 using an antibody specific for the C terminus of GAB2 or HA as a negative control. Immune complexes were immunoblotted with either the same antibody (*Upper*) or an antibody recognizing the first N-terminal 39 aa (*Lower*).

